diabetes®
American Diabetes Association®

Alterations in Adipose Tissue Distribution, Cell Morphology, and Function Mark Primary Insulin Hypersecretion in Youth With Obesity

Domenico Tricò, Martina Chiriacò, Jessica Nouws, Alla Vash-Margita, Romy Kursawe, Elena Tarabra, Alfonso Galderisi, Andrea Natali, Cosimo Giannini, Marc Hellerstein, Ele Ferrannini, and Sonia Caprio

Diabetes 2024;73(6):941–952 | https://doi.org/10.2337/db23-0450

Metabolic Crosstalk Between β-Cells and Adipocytes in Youth With Obesity and Primary Insulin Hypersecretion

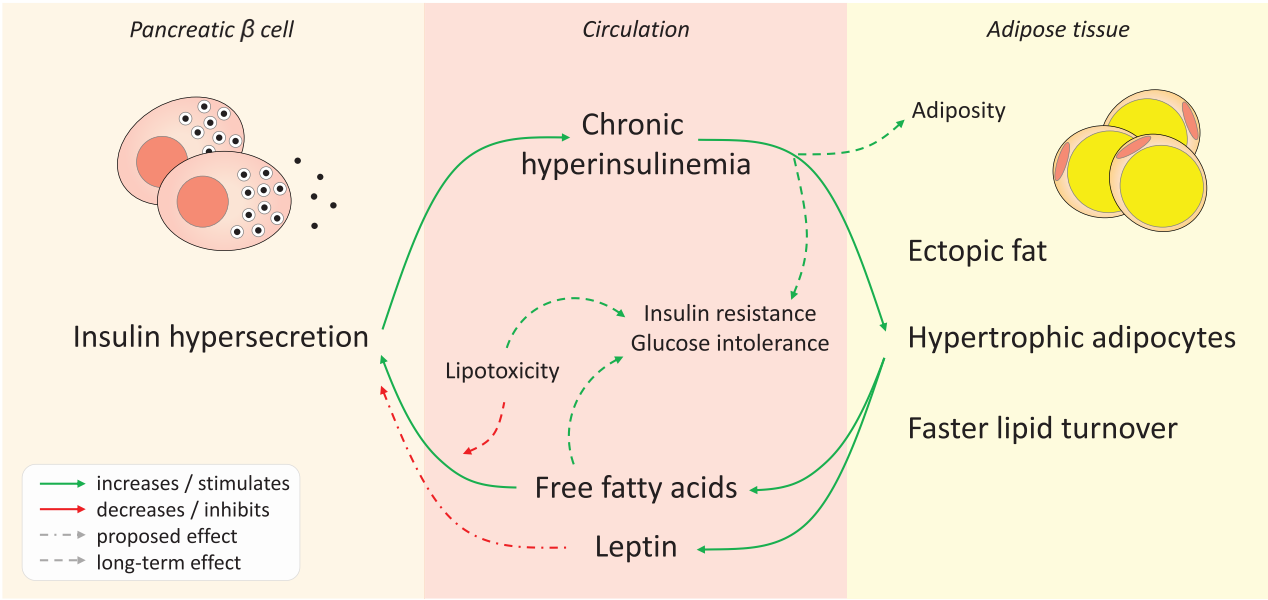

Alterations in Adipose Tissue Distribution, Cell Morphology, and Function Mark Primary Insulin Hypersecretion in Youth With Obesity

Domenico Tricò,[1,2] Martina Chiriacò,[1,2] Jessica Nouws,[3] Alla Vash-Margita,[4] Romy Kursawe,[5] Elena Tarabra,[6] Alfonso Galderisi,[3] Andrea Natali,[1,2] Cosimo Giannini,[7] Marc Hellerstein,[8] Ele Ferrannini,[9] and Sonia Caprio[3]

Diabetes 2024;73:941–952 | https://doi.org/10.2337/db23-0450

Excessive insulin secretion independent of insulin resistance, defined as primary hypersecretion, is associated with obesity and an unfavorable metabolic phenotype. We examined the characteristics of adipose tissue of youth with primary insulin hypersecretion and the longitudinal metabolic alterations influenced by the complex adipoinsular interplay. In a multiethnic cohort of adolescents with obesity but without diabetes, primary insulin hypersecretors had enhanced model-derived β-cell glucose sensitivity and rate sensitivity but worse glucose tolerance, despite similar demographics, adiposity, and insulin resistance measured by both oral glucose tolerance test and euglycemic-hyperinsulinemic clamp. Hypersecretors had greater intrahepatic and visceral fat depots at abdominal MRI, hypertrophic abdominal subcutaneous adipocytes, higher free fatty acid and leptin serum levels per fat mass, and faster in vivo lipid turnover assessed by a long-term ^2H_2O labeling protocol. At 2-year follow-up, hypersecretors had greater fat accrual and a threefold higher risk for abnormal glucose tolerance, while individuals with hypertrophic adipocytes or higher leptin levels showed enhanced β-cell glucose sensitivity. Primary insulin hypersecretion is associated with marked alterations in adipose tissue distribution, cellularity, and lipid dynamics, independent of whole-body adiposity and insulin resistance. Pathogenetic insight into the metabolic crosstalk between β-cell and adipocyte may help to identify individuals at risk for chronic hyperinsulinemia, body weight gain, and glucose intolerance.

ARTICLE HIGHLIGHTS

- Excessive insulin secretion independent of insulin resistance, named primary hypersecretion, has been associated with obesity and glucose intolerance.
- We examined whether early alterations in adipose tissue phenotype and function are linked to primary insulin hypersecretion in a complex interplay influencing glucose tolerance, β-cell function, and adiposity.
- In adolescents with obesity, insulin hypersecretors have greater ectopic fat depots, hypertrophic adipocytes, higher leptin and free fatty acid levels per fat mass, and greater lipid turnover than normosecretors.
- Hypertrophic adipocytes and hyperleptinemia predict short-term increases in β-cell glucose sensitivity, while the hypersecretory phenotype identifies individuals at risk of glucose intolerance and accruing adiposity over time.

The pathological sequence leading to obesity-related type 2 diabetes (T2D) is incompletely known, thereby hindering

[1]Department of Clinical and Experimental Medicine, University of Pisa, Pisa, Italy
[2]Laboratory of Metabolism, Nutrition, and Atherosclerosis, University of Pisa, Pisa, Italy
[3]Department of Pediatrics, Yale School of Medicine, New Haven, CT
[4]Department of Obstetrics, Gynecology and Reproductive Sciences, Yale School of Medicine, New Haven, CT
[5]The Jackson Laboratory for Genomic Medicine, Farmington, CT
[6]Alexion Pharmaceuticals, Inc., New Haven, CT
[7]Department of Pediatrics, University of Chieti "G. d'Annunzio," Chieti, Italy
[8]Department of Nutritional Sciences and Toxicology, University of California, Berkeley, Berkeley, CA
[9]Institute of Clinical Physiology, National Research Council, Pisa, Italy

Corresponding authors: Domenico Tricò, domenico.trico@unipi.it, and Sonia Caprio, sonia.caprio@yale.edu

Received 8 June 2023 and accepted 16 October 2023

Clinical trial reg. no. NCT03195400, clinicaltrials.gov

This article contains supplementary material online at https://doi.org/10.2337/figshare.24354253.

See accompanying article, p. 837.

the development of targeted preventive strategies to mitigate the growing incidence and socioeconomic burden of the disease (1). Chronic hyperinsulinemia due to excess insulin secretion has been postulated as the primum movens of T2D, preceding and leading to insulin resistance, β-cell exhaustion, and ultimately dysglycemia (2–9). We previously demonstrated that adolescents and adults with normal glucose tolerance (NGT) and an inappropriate insulin secretion that more than compensates for the degree of insulin resistance, defined as primary insulin hypersecretion, have a worse metabolic profile and increased risk of progression to dysglycemia over time (10). Furthermore, the Restoring Insulin Secretion (RISE) study revealed that youth with impaired glucose tolerance (IGT) or recently diagnosed T2D have greater insulin responses for any degree of insulin resistance compared with adults, despite similar glucose tolerance, which may contribute to a more rapid β-cell failure regardless of pharmacological treatment (11,12). However, the role of primary hyperinsulinemia in the early disease course is yet to be established (13), and further studies are needed to define the mechanisms of β-cell overstimulation in the absence of insulin resistance and glucose dysregulation.

Excess circulating substrates, including free fatty acids (FFAs) (14–17) and their precursors triglycerides (TGs) (18–20), can overstimulate the β-cell to increase fasting and postprandial insulin secretion. In turn, prolonged hyperinsulinemia can lead to weight gain and increased adiposity, particularly in youth (21). A recent study suggested that obesity itself stimulates insulin secretion, independent of insulin resistance and glucose tolerance (9). The adipose tissue is devoted to the storage and release of lipids and when in excess, can induce insulin hyperresponsiveness via increased release of both FFAs (17) and adipocyte-derived hormones (named adipokines), including leptin and adiponectin (22–24). Although adipose tissue accumulates predominantly as subcutaneous adipose tissue (SAT), other fat depots like visceral adipose tissue (VAT) and intrahepatic fat are abundant in individuals with obesity, thereby influencing insulin clearance (25) and possibly secretion (26,27). During weight gain, adipose depots expand through an increase in adipocyte size and/or number. Enlarged adipocytes, typically observed in obesity, are less susceptible to insulin's antilipolytic action (28) and show increased leptin release (29,30). Furthermore, adipocyte size strongly correlates with insulin levels, independent of BMI or fat mass (FM) (31,32).

To gain a better understanding of the complex metabolic crosstalk between β-cells and adipocyte cellularity/endocrine function, we examined the metabolic phenotype of primary insulin hypersecretors in a multiethnic cohort of adolescents with obesity by *1*) measuring β-cell function and insulin sensitivity via euglycemic-hyperinsulinemic clamp and 3-h, frequently sampled oral glucose tolerance test (OGTT) with C-peptide/glucose modeling; *2*) measuring fat depot distribution and intrahepatic fat via abdominal MRI; *3*) assessing adipocyte morphology in abdominal SAT biopsies; *4*) measuring dynamic fluxes of adipose TGs and de novo lipogenesis (DNL) in vivo using long-term ^2H_2O labeling; and *5*) analyzing the trajectories and mutual influence of β-cell function and adiposity over time via longitudinal metabolic assessments.

RESEARCH DESIGN AND METHODS

Study Participants

The Yale Pathogenesis of Youth-Onset Type 2 Diabetes (PYOD) study is a long-term project aimed at examining early alterations in glucose homeostasis in relation to body fat patterns in children and adolescents with obesity (age 7–21 years, BMI ≥85th percentile for age and sex). Exclusion criteria included any relevant medical therapy or condition affecting glucose and lipid metabolism, including alcohol consumption and smoking. A detailed medical and family history was obtained from all participants, and a physical examination was performed by a trained pediatrician. Tanner stage was determined by a pediatric endocrinologist based on breast development in girls and genitalia development in boys. All participants underwent a 3-h, frequently sampled OGTT; anthropometric measurements, including total body composition by DEXA scan; and an accurate assessment of abdominal fat distribution by MRI. After enrollment, participants received standard nutritional guidance as well as recommendations for physical activity and were scheduled to be followed up every 4–6 months according to routine clinical practice. One hundred participants agreed to have an abdominal SAT biopsy for the determination of adipocyte size at baseline and were included in this analysis. Subsets of these participants also underwent a euglycemic-hyperinsulinemic clamp, a long-term labeling protocol with ^2H_2O for the determination of lipid dynamics, and/or additional OGTTs and DEXA scans at follow-up, as detailed below. Characteristics of participant subsets are reported in Supplementary Tables 1–3.

The study was conducted according to the principles expressed in the Declaration of Helsinki and was approved by the Yale human investigation committee. All participants, or parents of minors, gave their written informed consent before enrollment.

Frequently Sampled OGTT

All participants underwent a 3-h, 75-g OGTT at baseline, and 68 participants returned for a follow-up OGTT after a median follow-up of 2 years. OGTTs were performed at the Yale Center for Clinical Investigation at 8:00 A.M. after an overnight fast. Before the test, participants were asked to follow a weight maintenance diet consisting of at least 250 g of carbohydrates daily for 7 days and to avoid intense physical activity. Baseline fasting blood samples were obtained for measurement of glucose, insulin, C-peptide, lipid profile, FFAs, adipokines, and routine biochemical analyses. Blood samples were taken every 10 min for the first 30 min, then

every 30 min until the end of the study to measure plasma glucose, insulin, and C-peptide levels.

In agreement with the current diagnostic criteria of the American Diabetes Association, NGT was defined as fasting and 120-min glucose values <5.6 mmol/L and <7.8 mmol/L, respectively; impaired fasting glucose (IFG) as fasting glucose between 5.6 and 6.9 mmol/L; and IGT as 120-min glucose between 7.8 and 11.0 mmol/L. Participants with repeated OGTTs were defined as progressors in the case of progression from NGT to IFG/IGT or persistence of IFG/IGT from the first to the second OGTT (33).

Euglycemic-Hyperinsulinemic Clamp

Fifty-nine participants underwent an euglycemic-hyperinsulinemic clamp at the Yale Center for Clinical Investigation at 7:30 A.M. after an overnight fast (Supplementary Table 1). An antecubital catheter was inserted for insulin and glucose intravenous infusion. Insulin was infused at a primed continuous infusion rate of 80 $mU \cdot m^{-2} \cdot min^{-1}$ for 120 min. The glucose infusion rate was adjusted every 5 min to reach and maintain a target plasma glucose value of 5.1 mmol/L (92 mg/dL) throughout the test.

Abdominal MRI and Body Composition

Abdominal MRI studies were performed on a Siemens Sonata 1.5-T system to quantify the area of VAT and SAT depots on a single slice obtained at the L4/L5 disc space level, as previously described (26). Hepatic fat fraction (HFF) was measured using an advanced magnitude-based liver fat quantification MRI technique, the two-point Dixon, as modified by Fishbein et al. (34) and validated against liver biopsy in adolescents with obesity (25,27). Total body composition was measured by DEXA using a Hologic scanner (Hologic, Boston, MA) in all participants at baseline and in the 68 participants in the longitudinal cohort.

Adipose Tissue Biopsy and Cell Size Analysis

All participants underwent a biopsy of the abdominal SAT according to a standard procedure (35) to measure adipocyte size and number. Two samples weighing 20–30 mg were fixed with osmium (Multisizer 3; Beckman Coulter, Miami, FL), and the adipose cell size distribution was determined using a curve-fitting analysis (Supplementary Fig. 1), as previously described (36). The peak diameter was identified as the mean diameter at which the frequency of the large cell population reached a maximum. The nadir diameter was defined as the mean cell diameter corresponding to the lowest point in frequency between the large and small cell populations. Thus, the two populations of small and large adipocytes were identified as the adipose cells with diameters below and above the nadir diameter, respectively. The number of large and small adipocyte cells were calculated as the percentage of large or small cells in SAT biopsies multiplied by the total number of cells, which was estimated based on the average cell and SAT volume for each individual (37).

Lipid Dynamics by ^2H_2O Labeling

A total of 17 participants underwent an 8-week ^2H_2O labeling protocol prior to SAT biopsy (Supplementary Table 2), as previously detailed (35). Participants drank varying daily amounts of 70% ^2H_2O to achieve a plateau in ^2H_2O body enrichment, and their body weight was closely monitored to avoid weight gain or changes in FM. The Folch technique was used to isolate TGs from SAT adipocytes (38). Incorporation of deuterium (^2H) from ^2H_2O into TG-glycerol from all-source TG synthesis was measured to assess the net newly synthesized TG retained in SAT during the labeling period (TG turnover). ^2H incorporation into TG-palmitate was measured as a marker of DNL. TG-glycerol and TG-palmitate were measured by gas chromatography mass spectrometry and mass isotopomer distribution analysis (35).

Biochemical Analyses

Plasma glucose was determined at bedside during both OGTT and clamp with the glucose oxidase method (Beckman Instruments, Brea, CA). Plasma insulin, leptin, and adiponectin were measured by radioimmunoassays (Linco, St. Charles, MO). Plasma C-peptide was measured by ELISA using ALPCO immunoassays (Salem, NH). Lipid levels were determined with an autoanalyzer (model 747-200; Roche Diagnostic, Indianapolis, IN). Liver enzymes and FFAs were measured by using standard automated kinetic enzymatic assays. Plasma adipokine and FFA levels were adjusted for FM (kg) to provide an estimate of leptin, adiponectin, and FFA secretion per unit of adipose tissue. Plasma adipokine levels were also adjusted for the target tissue mass (i.e., lean body mass [LBM]).

Calculations

β-Cell Function and Insulin Clearance

The C-peptide deconvolution method was used to estimate the insulin secretion rate (ISR). β-Cell function was assessed from the OGTT using a validated mathematical model (39). Through the analysis of ISR and glucose concentrations, this model allows the determination of the following components: *1*) β-cell glucose sensitivity, which describes the dependence of ISR on absolute glucose concentration through a dose-response function, whose intercept at a fixed glucose level of 5 mmol/L is identified by the ISR@5; *2*) potentiation factor, which accounts for glucose- and nonglucose-mediated modulation of the ISR during the OGTT and is expressed as the ratio between values at 160–180 min and 0–20 min; and *3*) β-cell rate sensitivity, which describes the dynamic dependence of ISR on the rate of change of glucose concentration and is related to early insulin release.

Insulin clearance was calculated as the ratio between the areas under the curves of ISR and plasma insulin during the OGTT, calculated using the trapezoid rule (25). Fasting insulin clearance was calculated as the ratio between ISR and plasma insulin measured at fasting (25).

Insulin Sensitivity

Whole-body insulin sensitivity was estimated by the whole-body insulin sensitivity index (WBISI), calculated as 10,000/the square root of ([fasting glucose · fasting insulin] · [mean glucose · mean insulin during OGTT]), which was validated in obese adolescents against the euglycemic-hyperinsulinemic clamp (40). Insulin sensitivity was also measured as the glucose disposal rate (*M* value) during the last 30 min of the euglycemic-hyperinsulinemic clamp, expressed as mg of glucose infused per min per kg of LBM.

Hepatic insulin resistance was estimated by the liver insulin resistance index, calculated using an algorithm based on OGTT insulin levels, percent FM (FM%), BMI, and HDL cholesterol, which has been validated against tracer-derived measures of liver insulin resistance in individuals without diabetes (41).

Statistical Analysis

Continuous variables with normal and nonnormal distribution are presented as mean ± SD or median (interquartile range [IQR]), respectively. Nominal variables are reported as counts with percentages. Differences between independent groups were tested using Mann-Whitney *U* test for continuous variables and Fisher exact test for nominal variables. Cohen κ-coefficient was used to estimate the agreement between different classifications. The Wilcoxon signed rank test was used to test for changes in repeated measures. Logistic regression analysis was used to calculate odds ratios and 95% CIs.

Statistical analyses were performed using JMP Pro 16.0 software (SAS Institute, Cary, NC). A two-sided α-level of 0.05 was considered significant. A complete case analysis approach was used to account for any missing data. Graphical representations were created using GraphPad Prism 8.4.3 software (GraphPad Software, La Jolla, CA).

Data and Resource Availability

The data sets generated and/or analyzed during the current study are available from the corresponding authors upon reasonable request.

RESULTS

Study Cohort

The study population consisted of 100 adolescents of various ethnicities/races from the PYOD study who were overweight or obese and free of diabetes (age 15.8 ± 2.7 years, 39 girls, BMI *z* score 2.2 [IQR 2.0–2.6]). Their main and metabolic clinical characteristics are reported in Table 1.

Identification of Primary Insulin Hypersecretors

Primary insulin hypersecretion was defined based on the residuals' distribution of the best fit line (log-log) between total ISR and WBISI during a 3-h OGTT (10). The participants belonging to the upper tertile of the residuals' distribution were classified as having insulin hypersecretion (HyperS) (n = 33), whereas participants in the middle and lower tertile were classified as having normal insulin secretion (NormS) (n = 67) (Fig. 1*A*). This classification showed an almost perfect level of agreement (κ = 0.809) with the classification based on the *M* value measured during the euglycemic-hyperinsulinemic clamp (available for 59 of 100 participants) (Supplementary Table 1), with WBISI and *M* value being strongly correlated (r = 0.79, $P < 0.0001$).

Metabolic Phenotype of Primary Insulin Hypersecretors

Participants with HyperS and NormS had similar demographic and anthropometric characteristics, lipid profiles, and liver enzymes (Table 1). Fasting plasma glucose was slightly higher in participants with NormS than those with HyperS, despite similar insulin levels. Conversely, 2-h and mean plasma glucose and insulin levels during the OGTT were higher in the HyperS group (Fig. 1*B* and *C*). According to the classification criteria, both fasting and glucose-stimulated ISR were markedly higher in the HyperS compared with the NormS group (21% and 62%, respectively) (Fig. 1*D–F*). Among model-derived parameters of β-cell secretory function, participants with HyperS showed a 36% higher β-cell glucose sensitivity, 49% higher ISR@5, and 71% higher β-cell rate sensitivity, indicating enhanced static and dynamic β-cell response to glucose, with no difference in the potentiation factor (Fig. 1*G–J*). Insulin clearance during the OGTT (Fig. 1*K*) and whole-body insulin sensitivity assessed by either WBISI (Fig. 1*L*) or *M* value (Table 1) were similar between groups, while both hepatic insulin resistance index (Table 1) and fasting insulin clearance (1.05 [IQR 0.86–1.36] vs. 0.83 [0.70–1.02] $L \cdot min^{-1} \cdot m^{-2}$, P = 0.001) were higher in the HyperS than NormS group.

Abdominal Fat Distribution

Participants with HyperS and NormS had similar degrees of adiposity as measured by DEXA scan (Table 1) and abdominal MRI (Fig. 2*A* and *B*). However, the HyperS group showed a 34% higher VAT proportion (VAT/[VAT + SAT]) and a threefold higher HFF compared with the NormS group (Fig. 2*C* and *D*).

Adipocyte Cell Morphology

The size distribution profile of adipocytes from the abdominal SAT depot demonstrated a hypertrophic phenotype of the large adipocyte population in participants with HyperS, characterized by enlarged cell size and reduced cell number. In participants with HyperS, the peak and nadir diameters of the large cell population were 6.0% and 7.5% larger, respectively, compared with participants with NormS (Fig. 2*E* and *F*), while the number of large adipocytes was significantly lower (393 [IQR 324–530] · 10^6 vs. 570 [374–849] · 10^6 cells, P = 0.008). The number of small adipocytes (376 [278–717] · 10^6 vs. 430 [278–615] · 10^6 cells, P = 0.725) and the mean cell size (86 [75–91] vs. 83 [75–94] μm, P = 0.698) did not differ between groups.

Table 1—Participant characteristics

	Whole cohort (*N* = 100)	HyperS (*n* = 33)	NormS (*n* = 67)	*P*
Age, years	15.8 ± 2.7	15.6 ± 2.5	16.0 ± 2.7	0.365
Girls	39 (39.0)	9 (27.3)	30 (44.8)	0.127
Race and ethnicity				0.345
Non-Hispanic Black	35 (35)	13 (39.4)	22 (32.8)	
Non-Hispanic White	32 (32)	11 (33.3)	21 (31.3)	
Hispanic	30 (30)	7 (21.2)	23 (34.3)	
Other	3 (3)	2 (6.1)	1 (1.5)	
Tanner stage				0.515
I	5 (5.0)	1 (3.0)	4 (6.0)	
II–III	24 (24.0)	10 (30.3)	14 (20.9)	
IV–V	71 (71.0)	22 (66.7)	49 (73.1)	
Body weight, kg	100.7 (83.7–118.1)	91.0 (79.7–111.1)	101.8 (85.6–123.0)	0.106
BMI *z* score, kg/m^2	2.2 (2.0–2.6)	2.2 (1.9–2.5)	2.3 (2.0–2.7)	0.136
FM%	42.5 ± 10.1	40.7 ± 8.2	41.9 ± 9.2	0.489
LBM, kg	55.2 ± 11.3	52.8 ± 11.3	56.4 ± 11.3	0.133
Waist circumference, cm	108.2 ± 18.2	106.0 ± 12.2	109.3 ± 20.6	0.342
Waist-to-hip ratio	0.92 ± 0.08	0.93 ± 0.07	0.92 ± 0.09	0.409
Total cholesterol, mg/dL	147 (132–174)	153 (123–174)	147 (139–175)	0.890
HDL cholesterol, mg/dL	38 (30–45)	41 (35–48)	44 (35–52)	0.467
LDL cholesterol, mg/dL	87 (70–108)	85 (65–111)	88 (74–107)	0.567
Triglycerides, mg/dL	90 (52–129)	98 (73–156)	86 (52–135)	0.096
FFA, μmol/L	485 (364–679)	524 (369–713)	467 (359–653)	0.180
Leptin, ng/mL	37 (23–57)	36 (30–68)	37 (21–56)	0.207
Adiponectin, ng/mL	6.0 (4.4–8.6)	5.1 (4.2–8.2)	6.2 (5.0–8.6)	0.188
Fasting glucose, mmol/L	5.1 ± 0.6	5.0 ± 0.4	5.3 ± 0.6	**0.017**
2-h Glucose, mmol/L	6.6 ± 1.6	7.0 ± 1.2	6.4 ± 1.7	**0.046**
Mean glucose, mmol/L	6.7 ± 1.3	7.0 ± 0.9	6.6 ± 1.4	**0.026**
IFG/IGT	13 (13.0)	9 (27.3)	8 (11.9)	0.087
Fasting insulin, pmol/L	150 (108–224)	141 (105–233)	150 (111–225)	0.857
Mean insulin, pmol/L	641 (457–962)	903 (516–1,368)	579 (426–808)	**0.004**
HOMA of insulin resistance	6.0 (4.0–9.8)	5.5 (3.8–9.7)	6.1 (4.0–9.8)	0.595
WBISI	1.9 (1.3–2.8)	1.7 (1.0–2.4)	1.9 (1.3–2.8)	0.200
M value[a], mg · kg$_{LBM}^{-1}$ · min^{-1}	4.73 (3.67–9.40)	4.34 (3.38–8.58)	5.34 (3.75–10.12)	0.131
Liver insulin resistance index	2.64 (2.41–2.81)	2.69 (2.56–2.92)	2.53 (2.38–2.76)	**0.005**
ALT, units/L	16 (11–25)	16 (12–33)	16 (10–24)	0.334
AST, units/L	20 (17–25)	21 (15–25)	19 (17–25)	0.701

Data are mean ± SD for normally distributed variables, median (IQR) for nonnormally distributed variables, and *n* (%) for categorical variables. Differences between HyperS and NormS were tested using Mann-Whitney *U* test for continuous variables or χ^2 test for categorical variables. $P \leq 0.05$ (indicated in boldface type) was considered statistically significant. [a]Available in 59 participants (HyperS, *n* = 19; NormS, *n* = 40).

Adipocyte Endocrine Function

The HyperS group showed 47% higher leptin levels normalized for FM compared with the NormS group (Fig. 2*G*), while both FM-adjusted adiponectin levels and the leptin/adiponectin ratio were similar between groups (Fig. 2*H* and *I*). Furthermore, the HyperS group showed 23% numerically higher leptin levels normalized for LBM compared with the NormS group (0.79 [IQR 0.60–1.21] vs. 0.64 [0.38–0.91] ng · mL^{-1} · kg$_{LBM}^{-1}$, $P = 0.053$), but similar LBM-adjusted adiponectin ($P = 0.457$) and leptin/

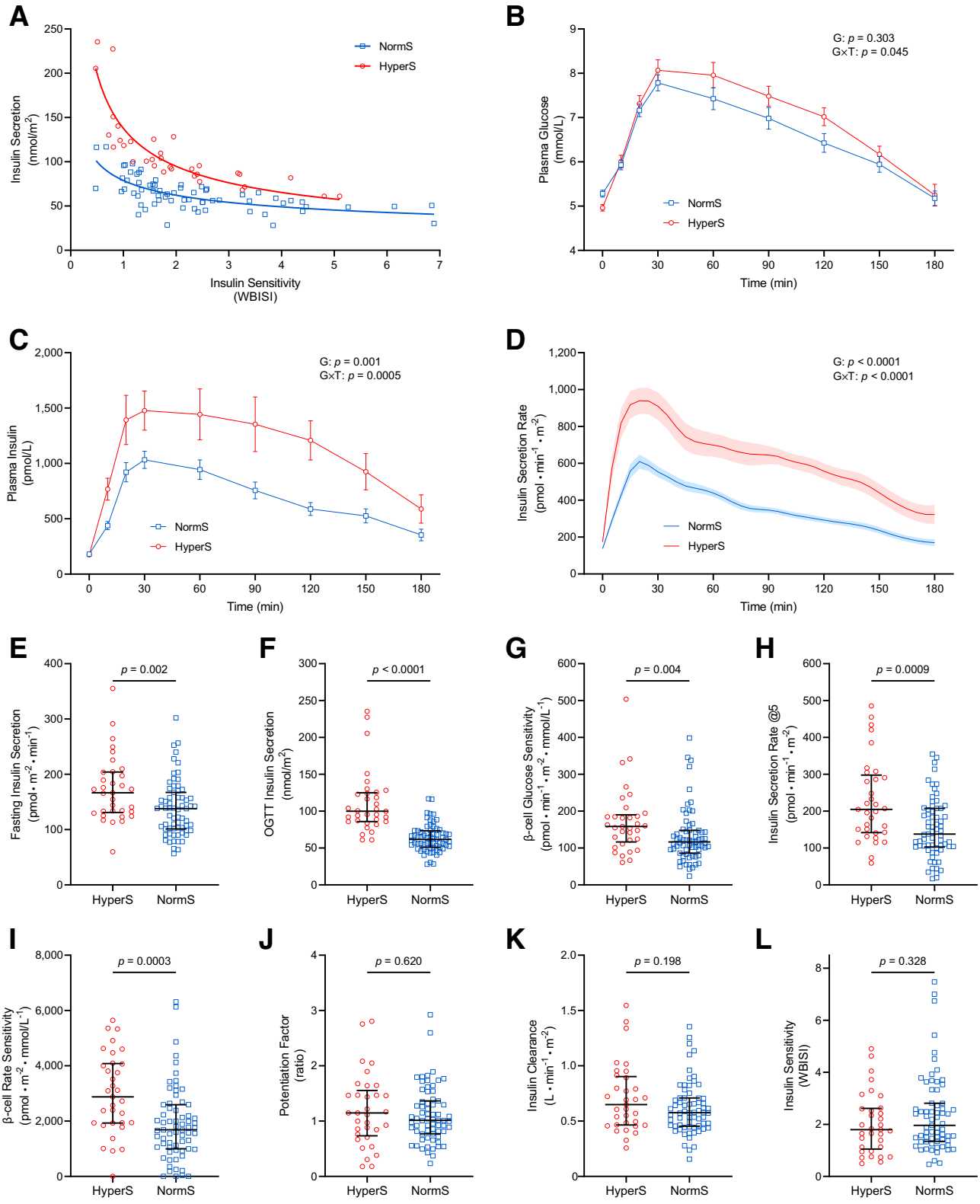

Figure 1—Glucose homeostatic mechanisms in participants with HyperS or NormS. *A*: Identification of participants with HyperS and NormS as the upper and middle-lower tertiles of the residuals' distribution of the OGTT-derived insulin secretion/WBISI best-fit line. *B–D*: Plasma glucose, insulin, and C-peptide–derived ISR profiles during the OGTT. *E* and *F*: Fasting and total insulin secretion. *G–J*: Model-derived β-cell glucose sensitivity, ISR@5, β-cell rate sensitivity, and potentiation factor ratio. *K* and *L*: Insulin clearance and WBISI. In *B–D*, data are mean ± SEM, and the group (G) and group-by-time interaction (G × T) effects were tested by two-way repeated-measures ANOVA. In *E–L*, lines represent median (IQR), and group differences were tested by Mann-Whitney *U* test.

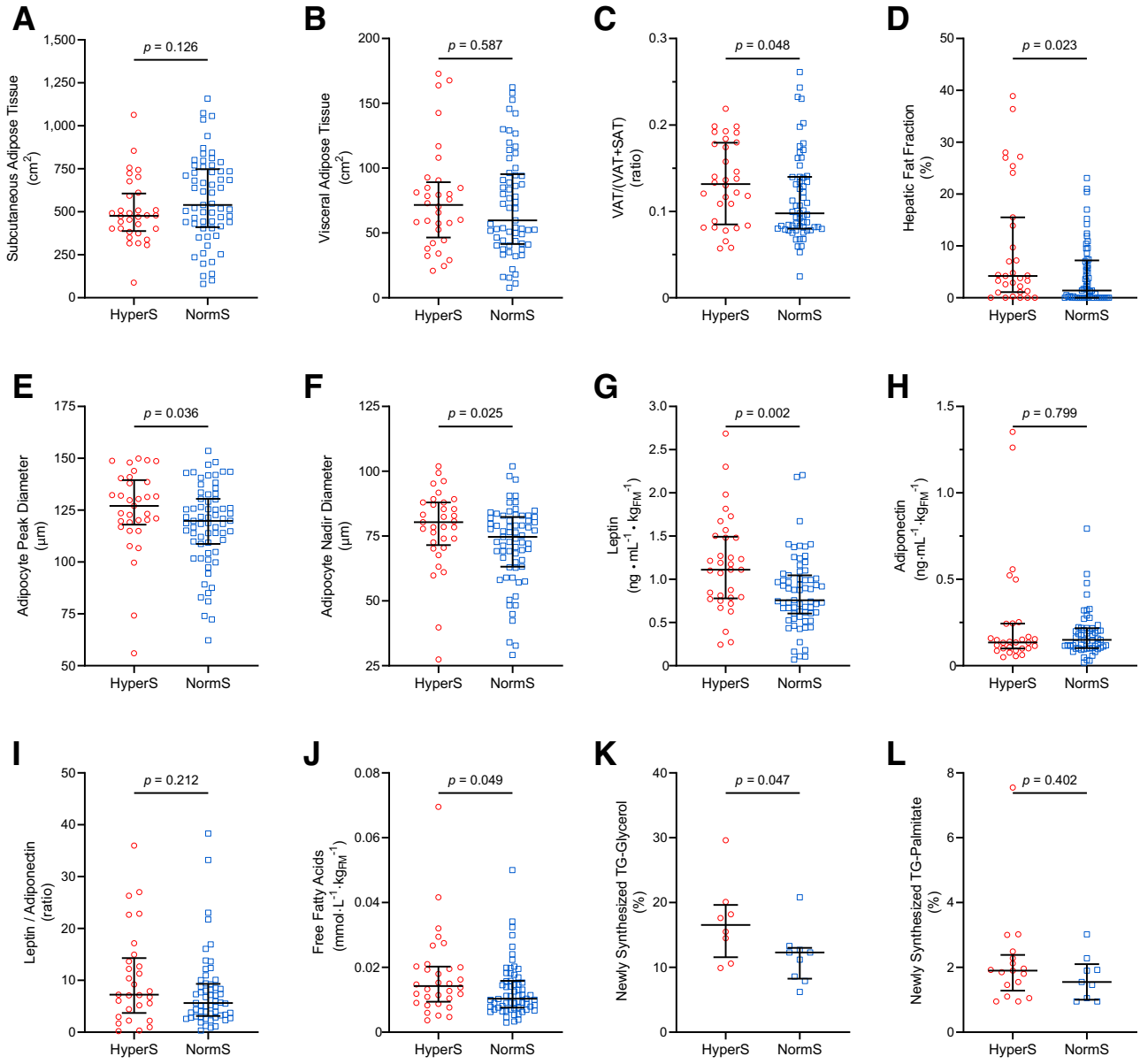

Figure 2—Adipose tissue distribution, morphology, and function in participants with HyperS or NormS. *A–D*: SAT, VAT, VAT proportion (VAT / [VAT + SAT]), and HFF by abdominal MRI. *E* and *F*: Peak diameter and nadir diameter of the large adipocyte population by curve-fitting analysis of SAT biopsies. *G–I*: Plasma leptin, adiponectin, and leptin-to-adiponectin ratio normalized by FM. *J*: Plasma FFAs normalized by FM. *K* and *L*: Newly synthesized TG-glycerol and TG-palmitate by ^2H_2O labeling. Lines represent median (IQR). Group differences were tested using Mann-Whitney *U* test.

adiponectin ratio ($P = 0.267$). Correlation analyses between plasma leptin and either FM or LBM in the HyperS and NormS groups are shown in Supplementary Fig. 2.

In Vivo Lipid Dynamics

Fasting FFA levels normalized to FM were higher in the HyperS than NormS group (Fig. 2*J*). Correlation analyses between plasma FFA and either FM or LBM in participants with HyperS and NormS are shown in Supplementary Fig. 3. To assess in vivo lipid dynamics, a subset of participants ($n = 17$) underwent a long-term ^2H_2O labeling protocol prior to SAT biopsy (Supplementary Table 2). Participants with HyperS showed accelerated TG turnover, as indicated by a 35% higher percentage of newly synthesized, ^2H_2O-labeled TG-glycerol. Fractional DNL, indicated by newly synthesized TG-palmitate, was similar between groups (Fig. 2*K* and *L*).

Longitudinal Effect of Insulin Hypersecretion on Glucose Tolerance and Adiposity

Sixty-eight of the 100 participants returned after a median follow-up of 2.3 (IQR 2.0–3.4) years for a second OGTT (Supplementary Table 3). Total body weight increased on average by 8.0 ± 2.5 kg at the end of follow-up ($P = 0.002$), without significant group differences ($P = 0.372$), as

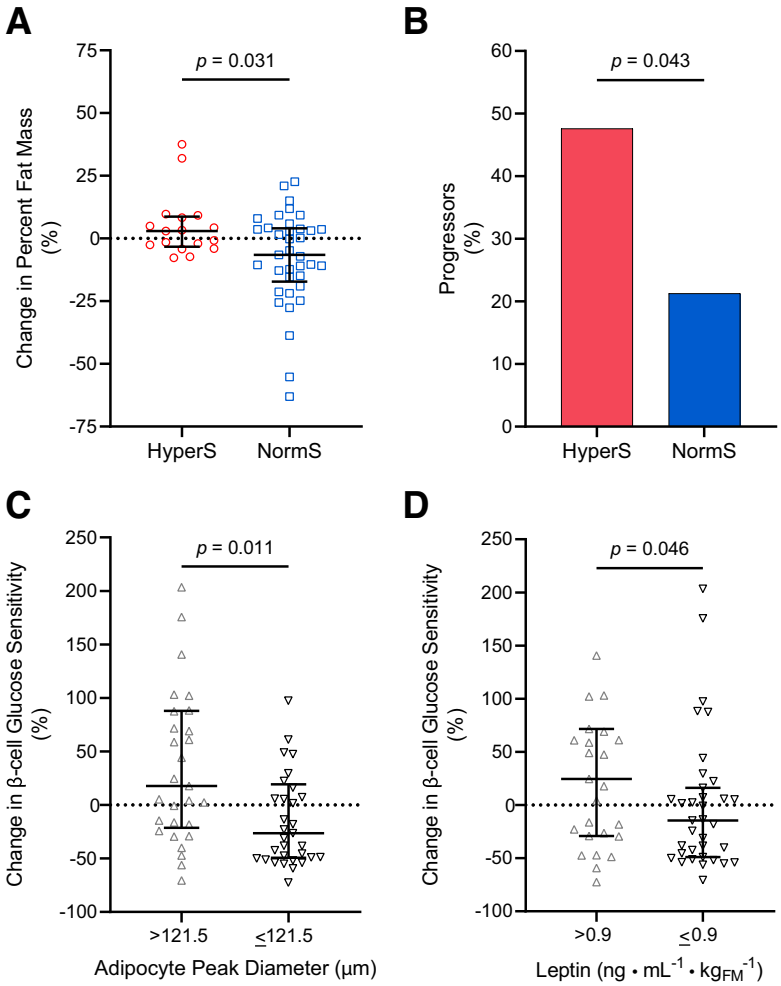

Figure 3—Longitudinal changes in FM, glucose tolerance, and β-cell function. *A* and *B*: Percent change in FM% and progression from NGT to IFG/IGT or persistence in the IFG/IGT phenotype of participants with HyperS or NormS. *C*: Percent change in model-derived β-cell glucose sensitivity in participants with adipocyte peak diameter above (>121.5 μm) or below (≤121.5 μm) the median. *D*: Percent change in model-derived β-cell glucose sensitivity in participants with plasma leptin levels above (>0.9 ng · mL^{-1} · kg_{FM}^{-1}) or below (≤0.9 ng · mL^{-1} · kg_{FM}^{-1}) the median. In *A*, *C*, and *D*, the lines represent the median (IQR), and group differences were tested using Mann-Whitney *U* test. In *B*, group differences were tested using Fisher exact test.

expected in growing youth. However, the BMI *z* score remained stable over time in both the participants with HyperS ($P = 0.329$) and NormS ($P = 0.954$). Total FM significantly increased in participants with HyperS (6.6 ± 2.5 kg, $P = 0.017$), while remaining stable in participants with NormS (−0.8 ± 2.2 kg, $P = 0.712$). Consistently, the degree of adiposity indicated by FM% was substantially unchanged in the HyperS group ($P = 0.170$) but significantly reduced in the NormS group ($P = 0.021$), leading to a 13% group difference in FM% percent change (Fig. 3*A*). Numerical differences between the HyperS and NormS groups in changes in WBISI (−0.6 [IQR −0.7 to 0.3] vs. 0.4 [−0.4 to 1.0], respectively, $P = 0.110$) and β-cell glucose sensitivity (−24 [−67 to 85] vs. 6 [−55 to 54] pmol · min^{-1} · m^{-2} · $mmol/L^{-1}$, $P = 0.901$) did not reach statistical significance.

Ten participants with HyperS (48%) and 10 participants with NormS (21%) were identified as progressors, with those with HyperS having a threefold greater odds for IFG/IGT at follow-up compared with those with NormS (odds ratio 3.36 [95% CI 1.11–10.16], $P = 0.043$) (Fig. 3*B*). Progressors showed a significant worsening in WBISI over time compared with nonprogressors (−0.5 [−0.9 to 0.1] vs. 0.5 [−0.2 to 1.1], respectively, $P = 0.0002$), whose extent was similar in HyperS and NormS progressors (−0.3 [−0.9 to 0.1] vs. −0.5 [−1.8 to 0], $P = 0.462$). Changes in β-cell glucose sensitivity were similar between progressors and nonprogressors in the whole longitudinal cohort ($P = 0.231$) and in the HyperS ($P = 0.637$) and NormS ($P = 0.919$) groups.

Longitudinal Effect of Adipocyte Characteristics on β-Cell Function

To investigate the relationships between the main adipocyte characteristics and the longitudinal changes in β-cell function, the participants of the original cohort were stratified based on the median adipocyte peak diameter (121.5 μm) and

leptin levels (0.9 ng · mL^{-1} · kg_{FM}^{-1}). β-Cell glucose sensitivity numerically increased over time in participants with larger adipocytes (P = 0.103) and numerically decreased in those with smaller adipocytes (P = 0.053), leading to a significant 44% group difference in β-cell glucose sensitivity percent change (Fig. 3*C*). Similarly, β-cell glucose sensitivity numerically increased in participants with higher leptin levels (P = 0.126) and numerically decreased in those with lower leptin levels (P = 0.102), leading to a significant 39% group difference in β-cell glucose sensitivity percent change (Fig. 3*D*).

DISCUSSION

In a multiethnic cohort of youth with obesity extensively characterized for glucose tolerance and main glucose homeostatic mechanisms, including model-derived insulin secretion and β-cell function parameters, insulin clearance, and OGTT- and clamp-derived insulin sensitivity, we identified individuals with an augmented oral glucose-stimulated insulin secretion that more than compensated for the degree of insulin resistance. These participants, classified as primary insulin hypersecretors, showed greater ectopic fat depots at abdominal MRI, enlarged adipocytes from SAT biopsies, higher leptin and FFA serum levels per FM, and greater lipid turnover as assessed by a long-term ^2H_2O labeling protocol, despite similar demographics, adiposity, and insulin resistance, compared with normosecretors. Notably, the hypersecretory phenotype showed worsening glucose tolerance and accruing adiposity in longitudinal assessments. In turn, hypertrophic adipocytes and high leptin levels at baseline predicted increases in β-cell glucose sensitivity over time. These results are consistent with the hypothesis of a complex adipo-insular axis mutually influencing the trajectories of glucose tolerance, β-cell function, and adiposity, whose earliest alterations could promote chronic hyperinsulinemia and progression to T2D in populations at risk.

Chronic hyperinsulinemia can induce body weight gain by inhibiting lipolysis and stimulating lipogenesis in adipose tissue, as supported by epidemiological (42–44) and intervention studies (45,46). In fact, the evidence that mice genetically incapable of sustained hyperinsulinemia (47–49) or with fat-specific insulin receptor knockout (50) are protected against diet-induced obesity strongly corroborates the causal role for hyperinsulinemia in obesity (51). In turn, fat buildup and obesity lead to ectopic fat accumulation in visceral depots and the liver, whose detrimental effects on glucose homeostasis can further worsen hyperinsulinemia (52,53). VAT exhibits a higher rate of lipolysis compared with SAT, resulting in an excess of circulating FFAs. VAT abundance also positively correlates with first- and second-phase insulin secretion in adult patients with T2D, independently of BMI and SAT (54). In agreement with these observations, we found a greater MRI-determined VAT proportion in relation to the total abdominal fat depots in youth with insulin hypersecretion, as well as numerically higher FFA levels, which may contribute to β-cell overstimulation (17) along with other adipocyte-derived metabolites and hormones (55,56).

The preferential influx of FFAs from VAT into the liver via the portal circulation can promote intrahepatic fat accumulation and hepatic insulin resistance. Indeed, the current study provides the first direct evidence confirming a greater degree of liver steatosis, quantified by abdominal MRI, in individuals with primary insulin hypersecretion, which was previously proposed in adults and adolescents based on surrogate indexes (10). The current study also corroborates previous indirect evidence in support of the impaired suppression of endogenous glucose release during the OGTT as the principal mechanism for the worse glucose tolerance in primary insulin hypersecretors (10). Remarkably, intrahepatic fat and hepatic insulin resistance may further worsen hyperinsulinemia by reducing first-pass insulin clearance (25,57). This mechanism, demonstrated in a large cohort of adults, has not been confirmed in two independent cohorts of adolescents, including the present one (10). A plausible explanation relies on the higher degree of obesity and insulin resistance in the pediatric populations analyzed, showing markedly lower insulin clearance even among normosecretors (median insulin clearance 1.7 L · min^{-1} · m^{-2} in adults vs. 0.6 L · min^{-1} · m^{-2} in both cohorts of youth).

The expansion of adipose tissue is allowed by an increase in adipocyte number (hyperplasia) and size (hypertrophy). Hyperplastic growth appears only at early stages of adipose tissue development, leveling off during adolescence, while hypertrophy can occur later in life to increase fat storage capacity in response to overfeeding (58). In our study, the cell size distribution profile of abdominal SAT biopsies revealed fewer but larger adipocytes in participants classified as hypersecretors, in whom adipose hypertrophy prevails over hyperplasia. Furthermore, a larger adipocyte size at baseline was associated with short-term increases in β-cell glucose sensitivity, possibly perpetuating chronic hyperinsulinemia, which is noteworthy in a population where β-cell function generally deteriorates over time (12,59). These observations align with the current knowledge that hypertrophic adipocytes are less susceptible to insulin antilipolytic action and may provide a chronic FFA overload to the β-cell (28) to enhance insulin secretion (31,32).

Adipocyte size is also an important determinant of adipokine secretion (29), with leptin release being proportional to adipocyte diameter (60). Thus, the increased serum leptin levels observed in the HyperS group, independent of FM, are likely related to the hypertrophic adipocyte phenotype. A direct correlation between leptin levels and β-cell function, indirectly assessed from fasting glucose and insulin levels through the HOMA-β index, was previously reported in a large cohort of adolescents (61). Our study confirms this finding through more accurate measures of β-cell function and provides the first evidence of a longitudinal association between overstimulated leptin and insulin secretion. Hyperinsulinemia directly enhances leptin secretion by the adipose tissue, while leptin has been shown to inhibit insulin

production and secretion in some (62–65), but not all studies (22,23,66) likely because of indirect effects. Given that leptin and insulin exert opposite effects on lipolysis and lipogenesis, an inhibitory feedback of leptin on insulin secretion has been proposed as a protective mechanism against insulin-stimulated adipogenesis (67).

An increased adipose lipid turnover, resulting from faster lipogenesis and lipolysis, is an important factor for the long-term development of obesity (29) and may contribute to ectopic fat accrual and the associated metabolic derangements (35). Using an elaborate long-term ^2H_2O labeling protocol, we found that fractional ^2H incorporation into TG-glycerol from SAT biopsies (representing newly synthesized TG retained in adipocytes over the course of ^2H exposure) was significantly different between groups, with the HyperS group having higher turnover rates. The reduced capacity of SAT to retain stored TG reflects marked resistance to the insulin antilipolytic action, especially in the context of chronic hyperinsulinemia. In turn, increased lipolysis can be responsible for the altered fat distribution and β-cell overstimulation in participants with HyperS by increasing systemic FFA and glycerol availability. Interestingly, the two groups had a similar fractional DNL, which suggests that the increased TG turnover does not depend on newly synthesized fatty acids (i.e., increased lipogenesis stimulated by hyperinsulinemia) but mostly on fat from diet or liver.

This study provides novel insight into the relationships between adipocyte morphology and lipid turnover with metabolic parameters. It also corroborates the unfavorable role of primary insulin hypersecretion and chronic hyperinsulinemia on glucose homeostasis, largely supporting prior evidence (10). The contrasting observation of lower (rather than higher) fasting glucose levels in HyperS can be attributed to the markedly higher degree of liver insulin resistance in the previous youth cohort (10) compared with the current one. In the present study, portal hyperinsulinemia occurred in participants with HyperS even in response to low glucose values (as indicated by high ISR@5) and may still be able to restrain endogenous glucose production, at least in the fasting state, given that the difference in liver insulin resistance between the HyperS and NormS groups was rather small (∼6%). Indeed, the ISR@5 has been identified as the main determinant of fasting glucose homeostasis among β-cell parameters (68).

The main strengths of this study include the young age and multiethnic composition of the cohort, the accurate characterization of β-cell function using mathematical C-peptide modeling during frequently sampled OGTTs, the direct assessment of abdominal fat distribution by MRI, and the use of SAT biopsies and labeled water to assess adipocyte cell morphology and TG kinetics. Furthermore, longitudinal data are provided in support of the bidirectional pathogenetic link between overstimulated β-cell function and adipose tissue alterations. Several study limitations also must be acknowledged, including the small sample size in subset analyses, which warrants caution in the interpretation of negative findings, and the exclusion of youth with normal body weight, which confines the validity of current findings to the obese population. Glucose fluxes were not directly measured during the OGTT by means of multiple glucose tracers. This hindered the opportunity to establish whether less suppressed endogenous glucose release and/or faster intestinal glucose absorption (e.g., because of a more rapid gastric emptying or reduced first-pass splanchnic glucose uptake [69,70]) occurred in participants with primary insulin hypersecretion, leading to postprandial hyperglycemia. Moreover, we could not quantify the potential contribution of reduced glucose disposal in the HyperS versus NormoS group, which would be consistent with numerically lower *M* values in participants with available clamp data, and we could not obtain direct measures of liver insulin resistance. The use of two OGTT-derived estimates of insulin secretion and resistance for participant classification was mandated by the lack of an independent and direct measure of insulin resistance (*M* value) in those who refused to undergo the clamp. It is worth noting, however, that the two estimates derive from distinct C-peptide (ISR) and insulin (WBISI) measurements and that the classification based on the *M* value (available in most participants) showed an excellent level of agreement with the classification based on the WBISI.

In summary, the current study provides novel integrated insight into the complex metabolic interplay between β-cells and adipose tissue in a multiethnic cohort of youth with obesity. Primary insulin hypersecretion, independent of insulin resistance and adiposity, is associated with ectopic fat accumulation, adipose hypertrophy, higher FFA and leptin levels per FM, and faster lipid turnover and predicts progression to dysglycemia and FM gain. In turn, alterations in adipocyte size and secretory phenotype observed in hypersecretors can influence the trajectory of β-cell function over time, perpetuating the hyperinsulinemic status at least in the short term (i.e., until β-cell exhaustion eventually occurs). This metabolic phenotype embraces all the early alterations that precede the onset of obesity-related T2D, identifying individuals at increased metabolic risk who may benefit the most from targeted interventions.

Acknowledgments. The authors thank Dr. Andrea Mari (National Research Council, Padova, Italy) for providing the tools for β-cell function modeling and fruitful discussions. The authors also thank the patients and their families, as well as the Yale Center for Genome Analysis, and the Yale Center for Clinical Investigation and Hospital Research Unit.

Funding. S.C. is funded by National Institutes of Health (NIH) grants R01-HD-40787, R01-HD-28016, R01-DK-111038, and K24-HD-01464. This work was also made possible by National Institute of Diabetes and Digestive and Kidney Diseases (NIDDK) grant DK-045735 to the Yale Diabetes Endocrinology Research Center, National Center for Advancing Translational Sciences (NCATS) grant UL1-RR-024139, and by the NIH Roadmap for Medical Research.

The contents of this scientific contribution are solely the responsibility of the authors and do not necessarily represent the official views of the NIH.

Duality of Interest. No potential conflicts of interest relevant to this study were reported.

Author Contributions. D.T. contributed to the study design, data analysis, interpretation of results, and manuscript drafting and editing. M.C. contributed to the data analysis, interpretation of results, and drafting of the manuscript. J.N., A.V.-M., R.K., E.T., C.G., and M.H. contributed to the study design, data collection, and manuscript editing. A.G., A.N., and E.F. contributed to the study design, interpretation of results, and manuscript editing and critical revision. S.C. contributed funding and to the study design, data collection, interpretation of results, manuscript editing and critical revision, and study supervision. D.T. and S.C. are the guarantors of this work and, as such, had full access to all the data in the study and take responsibility for the integrity of the data and the accuracy of the data analysis.

References

1. GBD 2021 Diabetes Collaborators. Global, regional, and national burden of diabetes from 1990 to 2021, with projections of prevalence to 2050: a systematic analysis for the Global Burden of Disease Study 2021. Lancet 2023;402:203–234
2. Kekäläinen P, Sarlund H, Pyörälä K, Laakso M. Hyperinsulinemia cluster predicts the development of type 2 diabetes independently of family history of diabetes. Diabetes Care 1999;22:86–92
3. Carnethon MR, Palaniappan LP, Burchfiel CM, Brancati FL, Fortmann SP. Serum insulin, obesity, and the incidence of type 2 diabetes in black and white adults: the atherosclerosis risk in communities study: 1987-1998. Diabetes Care 2002;25:1358–1364
4. Dankner R, Chetrit A, Shanik MH, Raz I, Roth J. Basal state hyperinsulinemia in healthy normoglycemic adults heralds dysglycemia after more than two decades of follow up. Diabetes Metab Res Rev 2012;28:618–624
5. Page MM, Johnson JD. Mild suppression of hyperinsulinemia to treat obesity and insulin resistance. Trends Endocrinol Metab 2018;29:389–399
6. Pories WJ, Dohm GL. Diabetes: have we got it all wrong? Hyperinsulinism as the culprit: surgery provides the evidence. Diabetes Care 2012;35:2438–2442
7. Reed MA, Pories WJ, Chapman W, et al. Roux-en-Y gastric bypass corrects hyperinsulinemia implications for the remission of type 2 diabetes. J Clin Endocrinol Metab 2011;96:2525–2531
8. Corkey BE. Diabetes: have we got it all wrong? Insulin hypersecretion and food additives: cause of obesity and diabetes? Diabetes Care 2012;35:2432–2437
9. Mittendorfer B, Patterson BW, Smith GI, Yoshino M, Klein S. β Cell function and plasma insulin clearance in people with obesity and different glycemic status. J Clin Invest 2022;132:e154068
10. Tricò D, Natali A, Arslanian S, Mari A, Ferrannini E. Identification, pathophysiology, and clinical implications of primary insulin hypersecretion in nondiabetic adults and adolescents. JCI Insight 2018;3:e124912
11. RISE Consortium. Metabolic contrasts between youth and adults with impaired glucose tolerance or recently diagnosed type 2 diabetes: II. observations using the oral glucose tolerance test. Diabetes Care 2018;41:1707–1716
12. RISE Consortium; RISE Consortium Investigators. Effects of treatment of impaired glucose tolerance or recently diagnosed type 2 diabetes with metformin alone or in combination with insulin glargine on β-cell function: comparison of responses in youth and adults. Diabetes 2019;68:1670–1680
13. Esser N, Utzschneider KM, Kahn SE. Early beta cell dysfunction vs insulin hypersecretion as the primary event in the pathogenesis of dysglycaemia. Diabetologia 2020;63:2007–2021
14. Rebelos E, Seghieri M, Natali A, et al. Influence of endogenous NEFA on beta cell function in humans. Diabetologia 2015;58:2344–2351
15. Newsholme P, Cruzat V, Arfuso F, Keane K. Nutrient regulation of insulin secretion and action. J Endocrinol 2014;221:R105–R120
16. Crespin SR, Greenough WB 3rd, Steinberg D. Stimulation of insulin secretion by long-chain free fatty acids. A direct pancreatic effect. J Clin Invest 1973;52:1979–1984
17. Fryk E, Olausson J, Mossberg K, et al. Hyperinsulinemia and insulin resistance in the obese may develop as part of a homeostatic response to elevated free fatty acids: a mechanistic case-control and a population-based cohort study. EBioMedicine 2021;65:103264
18. Tricò D, Mengozzi A, Baldi S, et al. Lipid-induced glucose intolerance is driven by impaired glucose kinetics and insulin metabolism in healthy individuals. Metabolism 2022;134:155247
19. Natali A, Baldi S, Bonnet F, et al.; RISC Investigators. Plasma HDL-cholesterol and triglycerides, but not LDL-cholesterol, are associated with insulin secretion in non-diabetic subjects. Metabolism 2017;69:33–42
20. Tricò D, Natali A, Mari A, Ferrannini E, Santoro N, Caprio S. Triglyceride-rich very low-density lipoproteins (VLDL) are independently associated with insulin secretion in a multiethnic cohort of adolescents. Diabetes Obes Metab 2018;20:2905–2910
21. Erion KA, Corkey BE. Hyperinsulinemia: a cause of obesity? Curr Obes Rep 2017;6:178–186
22. Tanizawa Y, Okuya S, Ishihara H, Asano T, Yada T, Oka Y. Direct stimulation of basal insulin secretion by physiological concentrations of leptin in pancreatic beta cells. Endocrinology 1997;138:4513–4516
23. Shimizu H, Ohtani K, Tsuchiya T, et al. Leptin stimulates insulin secretion and synthesis in HIT-T 15 cells. Peptides 1997;18:1263–1266
24. Okamoto M, Ohara-Imaizumi M, Kubota N, et al. Adiponectin induces insulin secretion in vitro and in vivo at a low glucose concentration. Diabetologia 2008;51:827–835
25. Tricò D, Galderisi A, Mari A, et al. Intrahepatic fat, irrespective of ethnicity, is associated with reduced endogenous insulin clearance and hepatic insulin resistance in obese youths: a cross-sectional and longitudinal study from the Yale Pediatric NAFLD cohort. Diabetes Obes Metab 2020;22:1628–1638
26. Umano GR, Shabanova V, Pierpont B, et al. A low visceral fat proportion, independent of total body fat mass, protects obese adolescent girls against fatty liver and glucose dysregulation: a longitudinal study. Int J Obes 2019;43:673–682
27. Tricò D, Caprio S, Rosaria Umano G, et al. Metabolic features of nonalcoholic fatty liver (NAFL) in obese adolescents: findings from a multiethnic cohort. Hepatology 2018;68:1376–1390
28. Tchkonia T, Thomou T, Zhu Y, et al. Mechanisms and metabolic implications of regional differences among fat depots. Cell Metab 2013;17:644–656
29. Skurk T, Alberti-Huber C, Herder C, Hauner H. Relationship between adipocyte size and adipokine expression and secretion. J Clin Endocrinol Metab 2007;92:1023–1033
30. Lundgren M, Svensson M, Lindmark S, Renström F, Ruge T, Eriksson JW. Fat cell enlargement is an independent marker of insulin resistance and 'hyperleptinaemia'. Diabetologia 2007;50:625–633
31. Hoffstedt J, Arner E, Wahrenberg H, et al. Regional impact of adipose tissue morphology on the metabolic profile in morbid obesity. Diabetologia 2010;53:2496–2503
32. Stern JS, Batchelor BR, Hollander N, Cohn CK, Hirsch J. Adipose-cell size and immunoreactive insulin levels in obese and normal-weight adults. Lancet 1972;2:948–951
33. Galderisi A, Tricò D, Dalla Man C, et al. Metabolic and genetic determinants of glucose shape after oral challenge in obese youths: a longitudinal study. J Clin Endocrinol Metab 2020;105:534–542
34. Fishbein MH, Gardner KG, Potter CJ, Schmalbrock P, Smith MA. Introduction of fast MR imaging in the assessment of hepatic steatosis. Magn Reson Imaging 1997;15:287–293
35. Nouws J, Fitch M, Mata M, et al. Altered in vivo lipid fluxes and cell dynamics in subcutaneous adipose tissues are associated with the unfavorable pattern of fat distribution in obese adolescent girls. Diabetes 2019;68:1168–1177
36. McLaughlin T, Sherman A, Tsao P, et al. Enhanced proportion of small adipose cells in insulin-resistant vs insulin-sensitive obese individuals implicates impaired adipogenesis. Diabetologia 2007;50:1707–1715
37. Kursawe R, Eszlinger M, Narayan D, et al. Cellularity and adipogenic profile of the abdominal subcutaneous adipose tissue from obese adolescents: association with insulin resistance and hepatic steatosis. Diabetes 2010;59:2288–2296

38. Strawford A, Antelo F, Christiansen M, Hellerstein MK. Adipose tissue triglyceride turnover, de novo lipogenesis, and cell proliferation in humans measured with 2H2O. Am J Physiol Endocrinol Metab 2004;286:E577–E588
39. Mari A, Tura A, Gastaldelli A, Ferrannini E. Assessing insulin secretion by modeling in multiple-meal tests: role of potentiation. Diabetes 2002;51(Suppl.1): S221–226
40. Yeckel CW, Weiss R, Dziura J, et al. Validation of insulin sensitivity indices from oral glucose tolerance test parameters in obese children and adolescents. J Clin Endocrinol Metab 2004;89:1096–1101
41. Vangipurapu J, Stančáková A, Kuulasmaa T, et al.; EGIR-RISC Study Group. A novel surrogate index for hepatic insulin resistance. Diabetologia 2011;54:540–543
42. Odeleye OE, de Courten M, Pettitt DJ, Ravussin E. Fasting hyperinsulinemia is a predictor of increased body weight gain and obesity in Pima Indian children. Diabetes 1997;46:1341–1345
43. Chen YY, Wang JP, Jiang YY, et al. Fasting plasma insulin at 5 years of age predicted subsequent weight increase in early childhood over a 5-year period—the Da Qing Children Cohort Study. PLoS One 2015;10:e0127389
44. Xu C, Zhou G, Zhao M, et al. Bidirectional temporal relationship between obesity and hyperinsulinemia: longitudinal observation from a Chinese cohort. BMJ Open Diabetes Res Care 2021;9:e002059
45. Lustig RH, Greenway F, Velasquez-Mieyer P, et al. A multicenter, randomized, double-blind, placebo-controlled, dose-finding trial of a long-acting formulation of octreotide in promoting weight loss in obese adults with insulin hypersecretion. Int J Obes 2006;30:331–341
46. Alemzadeh R, Langley G, Upchurch L, Smith P, Slonim AE. Beneficial effect of diazoxide in obese hyperinsulinemic adults. J Clin Endocrinol Metab 1998;83:1911–1915
47. Mehran AE, Templeman NM, Brigidi GS, et al. Hyperinsulinemia drives diet-induced obesity independently of brain insulin production. Cell Metab 2012;16:723–737
48. Templeman NM, Clee SM, Johnson JD. Suppression of hyperinsulinaemia in growing female mice provides long-term protection against obesity. Diabetologia 2015;58:2392–2402
49. Templeman NM, Mehran AE, Johnson JD. Hyper-variability in circulating insulin, high fat feeding outcomes, and effects of reducing Ins2 dosage in male Ins1-null mice in a specific pathogen-free facility. PLoS One 2016;11:e0153280
50. Boucher J, Mori MA, Lee KY, et al. Impaired thermogenesis and adipose tissue development in mice with fat-specific disruption of insulin and IGF-1 signalling. Nat Commun 2012;3:902
51. Templeman NM, Skovsø S, Page MM, Lim GE, Johnson JD. A causal role for hyperinsulinemia in obesity. J Endocrinol 2017;232:R173–R183
52. Gastaldelli A, Miyazaki Y, Pettiti M, et al. Metabolic effects of visceral fat accumulation in type 2 diabetes. J Clin Endocrinol Metab 2002;87:5098–5103
53. Brøns C, Jensen CB, Storgaard H, et al. Impact of short-term high-fat feeding on glucose and insulin metabolism in young healthy men. J Physiol 2009;587:2387–2397
54. Huang H, Zheng X, Wen X, Zhong J, Zhou Y, Xu L. Visceral fat correlates with insulin secretion and sensitivity independent of BMI and subcutaneous fat in Chinese with type 2 diabetes. Front Endocrinol (Lausanne) 2023;14:1144834
55. Kulaj K, Harger A, Bauer M, et al. Adipocyte-derived extracellular vesicles increase insulin secretion through transport of insulinotropic protein cargo. Nat Commun 2023;14:709
56. Biondi G, Marrano N, Borrelli A, et al. adipose tissue secretion pattern influences β-cell wellness in the transition from obesity to type 2 diabetes. Int J Mol Sci 2022;23:5522
57. Bizzotto R, Tricò D, Natali A, et al. New insights on the interactions between insulin clearance and the main glucose homeostasis mechanisms. Diabetes Care 2021;44:2115–2123
58. Spalding KL, Arner E, Westermark PO, et al. Dynamics of fat cell turnover in humans. Nature 2008;453:783–787
59. Tricò D, McCollum S, Samuels S, et al. Mechanistic insights into the heterogeneity of glucose response classes in youths with obesity: a latent class trajectory approach. Diabetes Care 2022;45:1841–1851
60. Lönnqvist F, Nordfors L, Jansson M, Thörne A, Schalling M, Arner P. Leptin secretion from adipose tissue in women. Relationship to plasma levels and gene expression. J Clin Invest 1997;99:2398–2404
61. Hung YJ, Chu NF, Wang SC, et al. Correlation of plasma leptin and adiponectin with insulin sensitivity and beta-cell function in children - the Taipei Children Heart Study. Int J Clin Pract 2006;60:1582–1587
62. Seufert J, Kieffer TJ, Leech CA, et al. Leptin suppression of insulin secretion and gene expression in human pancreatic islets: implications for the development of adipogenic diabetes mellitus. J Clin Endocrinol Metab 1999; 84:670–676
63. Ahrén B, Havel PJ. Leptin inhibits insulin secretion induced by cellular cAMP in a pancreatic B cell line (INS-1 cells). Am J Physiol 1999;277: R959–R966
64. Leclercq-Meyer V, Considine RV, Sener A, Malaisse WJ. Do leptin receptors play a functional role in the endocrine pancreas? Biochem Biophys Res Commun 1996;229:794–798
65. Covey SD, Wideman RD, McDonald C, et al. The pancreatic beta cell is a key site for mediating the effects of leptin on glucose homeostasis. Cell Metab 2006;4:291–302
66. Pallett AL, Morton NM, Cawthorne MA, Emilsson V. Leptin inhibits insulin secretion and reduces insulin mRNA levels in rat isolated pancreatic islets. Biochem Biophys Res Commun 1997;238:267–270
67. Kieffer TJ, Habener JF. The adipoinsular axis: effects of leptin on pancreatic beta-cells. Am J Physiol Endocrinol Metab 2000;278:E1–E14
68. Mengozzi A, Tricò D, Nesti L, et al.; RISC Investigators. Disruption of fasting and post-load glucose homeostasis are largely independent and sustained by distinct and early major beta-cell function defects: a cross-sectional and longitudinal analysis of the Relationship between Insulin Sensitivity and Cardiovascular risk (RISC) study cohort. Metabolism 2020;105:154185
69. Jalleh RJ, Jones KL, Rayner CK, Marathe CS, Wu T, Horowitz M. Normal and disordered gastric emptying in diabetes: recent insights into (patho)physiology, management and impact on glycaemic control. Diabetologia 2022;65:1981–1993
70. Tricò D, Mengozzi A, Frascerra S, Scozzaro MT, Mari A, Natali A. Intestinal glucose absorption is a key determinant of 1-hour postload plasma glucose levels in nondiabetic subjects. J Clin Endocrinol Metab 2019;104:2131–2139